We are IntechOpen, the world's leading publisher of Open Access books Built by scientists, for scientists

4,800
Open access books available

122,000
International authors and editors

135M
Downloads

Our authors are among the

154
Countries delivered to

TOP 1%
most cited scientists

12.2%
Contributors from top 500 universities

CLARIVATE ANALYTICS BOOK CITATION INDEX INDEXED

WEB OF SCIENCE™

Selection of our books indexed in the Book Citation Index in Web of Science™ Core Collection (BKCI)

Interested in publishing with us?
Contact book.department@intechopen.com

Numbers displayed above are based on latest data collected.
For more information visit www.intechopen.com

6

Experimental and Theoretical Study of Low-Dimensional Iron Oxide Nanostructures

Jeffrey Yue, Xuchuan Jiang*, Yusuf Valentino Kaneti and Aibing Yu
School of Materials Science and Engineering, University of New South Wales, Sydney, Australia

1. Introduction

Iron oxide has many phases, including 16 pure phases (e.g., FeO, Fe_3O_4), 5 polymorphs of FeOOH (e.g., α-FeOOH, β-FeOOH) and 4 kinds of Fe_2O_3 (e.g., α-Fe_2O_3, γ-Fe_2O_3). Because of their unique properties (optical, electronic, magnetic), they have found many applications in the areas of catalysts, magnetic recording, sorbents, pigments, flocculants, coatings, gas sensors, lubrications, and biomedical applications (e.g., magnetic resonance imaging, drug delivery and therapy).

Many efforts have been made in the synthesis (co-precipitation, hydrothermal, micro-emulsion, and sol-gel method), structural characterization, and functional exploration, as well as fundamental understandings of iron oxide nanostructures. Despite some success, several challenges still exist regarding the synthesis, strcture, properties, and fundamental understanding of the iron oxides. the grand challenge is how to efficiently synthesize iron oxides with controlled morphology, size and functionality, and how to fundamentally understand the formation and growth mechanisms, structure, and interaction forces. Therefore, the development of simple but effective experimental and theoretical strategies to overcome the challenges is still imperative.

To fundamentally understand the nanoscale system, theoretical methods should exist. Computational modeling is one of the most important enabling techniques in nanotechnology and material research. It can increase the pace of discovery across the entire scientific scope, and reduce the cost in the development and commercialization of technologies and materials. Various computational approaches have been developed and used to predict the materials properties (e.g., electronic, magnetic, optical) at different length and time scales. For example, at an atomic scale, density functional theory (DFT) is widely used for binding energy calculation, while at a microscopic scale, molecular dynamics (MD) are able to provide insights into atomic/molecular systems.

This Chapter will give a brief overview of the experimental and theoretical methods conducted on iron oxide nanostructures, particularly for low-dimensional iron oxide nanoparticles. This includes: (i) several representative methods for iron oxides nanomaterials in Sections 2 and 3; (ii) surface modified iron oxide nanostructures by

* Corresponding Author

surfactants, polymers, silica or metals in Section 4; (iii) functional properties of such nanomaterials in gas sensing, catalysis, and biotechnology in Section 5. Moreover, in Section 6, the discussion will be extended to the theoretical modeling and simulation methods that can predict the formation and performance of nanomaterials, such as MD and DFT methods.

2. Iron oxide materials

Iron is the fourth most abundant element in the Earth's crust, and iron oxides are commonly found in nature and have become the most plentiful transition metal oxides (Morrissey and Guerinot, 2009; Ilani et al., 1999). The complicated phases and features of iron oxides have been listed in **Table 1**.

Some crystalline phases of iron oxides are not very stable and can convert into others. Much work has been conducted to convert akaganéite to hematite and/or magnetite phases to pursuit good performance in catalysis and gas sensing applications. Magnetite nanorods can be produced by the conversion of iron oxyhydroxides into a thermally stable structure of hematite by heating above 400 ^{o}C in air, or magnetite in a mixture of H_2 and Ar gas (Bomati-Miguel et al., 2008). Recently, our group has simplified the phase conversion procedures among the iron oxides. The iron oxyhydroxides can directly convert into magnetite by using hydrazine as a reducing agent, and the morphology was maintained. Using this method, magnetite nanorods could be directly synthesized from akaganéite rather than using hematite as an intermediate (Yue et al., 2010).

By using hydrazine, iron(III) ions can be reduced to iron(II). The change in coordination number to the iron atom will therefore transfer from Fe–OH to Fe–O following dehydration. The structure change caused by loss of H_2O will create pores or holes within the nanorod framework. Continuous reaction with hydrazine can form larger defects in the 1-D nanostructure, leading to the collapse of the framework. At the same time, the FeO_6 units will reconstruct into other crystals, and the broken fractions could fuse with neighboring particles to form larger ones. However, this does not happen to hematite because of its thermally stable structure under the considered conditions. The nature of such a conversion needs further investigation. Nevertheless, the proposed approach could be used for a controlled conversion of akaganéite to magnetite nanostructures (**Fig. 1**) without high-temperature treatment. These porous magnetic structures would find more applications in electronic and magnetic areas (Yue et al., 2011).

3. Synthesis methods

A variety of methods have been reported to synthesize iron oxide nanoparticles, including solid-state, liquid-phase, and gas-phase syntheses, as listed in **Table 2**. Among the synthesis approaches, liquid-phase synthesis is the most popular. The iron salts are highly soluble in water and different additives can be used in conjunction to modify the structure of the nanoparticles. Moreover, the liquid-phase synthesis is convenient for understanding ageing, recrystallization, and evolution into other shapes and sizes. It is also available for controlling experimental conditions in liquid (e.g., concentration, salt precursor, pH, temperature, surface modifiers). A few representative synthesis methods are briefly introduced in this Section, such as co-precipitation, hydrothermal and microemulsion.

Iron oxides	Crystallographic system	Crystallographic structural features	References
Goethite (α-FeOOH)	Orthorhombica = 0.9956 nm, b = 0.30215 nm and c = 0.4608 nm	3D-structure built up with $FeO_3(OH)$ octahedra spreading along the (010) direction, with each octahedron linked to eight neighbouring octahedral by four edges and three vertices. Oxygen atoms are in tetrahedral surroundings, either OFe_3H or OFe_3H (bond).	Cornell and Schwertmann, 1991; Cudennec and Lecerf, 2005
Akaganéite (β-FeOOH)	Monoclinic a = 1.056 nm, b = 0.3031 nm and c = 1.0483 nm	Double chains of edge linked Fe(O, OH) octahedral that share corners to form a framework containing large tunnels with square cross sections.	Cornell and Schuwertmann, 1991; Garcia et al., 2009
Lepidocrocite (γ-FeOOH)	Orthorhombic a = 0.3071 nm, b = 1.2520 nm and c = 0.3873 nm	Arrays of close cubic -packed anions (O^{2-}/OH^-) stacked along the [150] direction with Fe^{3+} ions occupying the octahedral interstices.	Cornell and Schuwertmann, 1991
Feroxyhyte (δ′-FeOOH)	Hexagonal a = 0.293 nm and c = 0.456 nm	Disordered hexagonally close-packed array of anions with Fe^{3+} ions distributed over half the octahedral sites in an orderly manner.	Cornell and Schuwertmann, 1991
Hematite (α-Fe_2O_3)	Hexagonal a= 0.5035 nm and c = 1.375 nm	Stacking of sheets of octahedrally (six-fold) coordinated Fe^{3+} ions. Between two close-packed layers of oxygen ions. Each oxygen ion is bonded to only two Fe ions.	Mohapatra and Anand,2010
Maghemite (γ-Fe_2O_3)	Cubic a= 0.83474 nm	Each cell of maghemite contains 32 O^{2-} ions, 21(1/3) Fe^{3+} ions and 2 (1/3) O vacancies. Eight cations occupy tetrahedral sites and the remaining cations are distributed over the octahedral sites. The vacancies are confined to octahedral sites.	Cornell and Schuwertmann, 1991; Weckler and Lutz, 1998
Magnetite (Fe_3O_4)	Cubic a = 0.8396 nm	Inverse spinel structure with a face-centered cubic cell based on 32 O^{2-} ions, regularly close-cubic packed along [111], with Fe^{2+} ions and half of the Fe^{3+} occupying the octahedral sites and the other half of Fe^{3+} ions, occupying the tetrahedral sites.	Cornell and Schuwertmann, 1991 Mohapatra and Anand,2010

Table 1. Complicated phases and polymorphs of iron oxides in nature

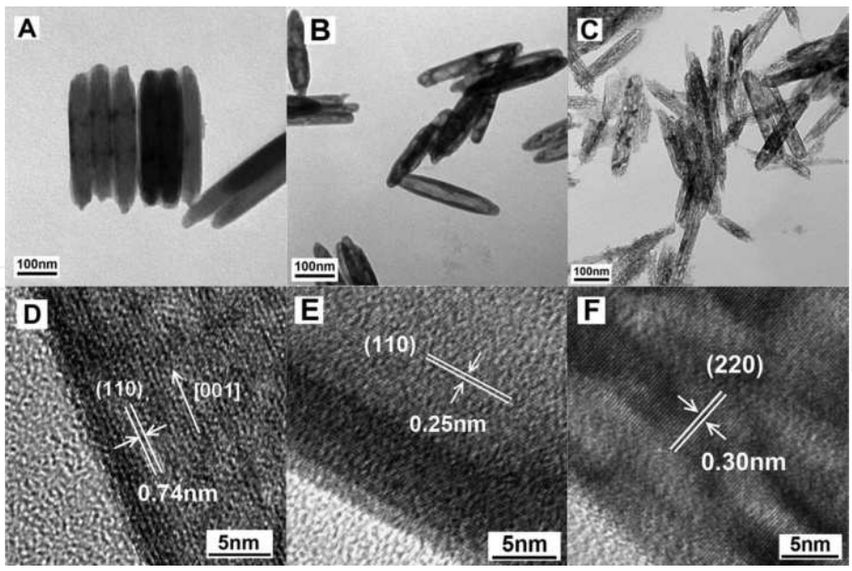

Fig. 1. TEM images showing the conversion of nanorods: (A) β-FeOOH nanorods, (B) β-FeOOH nanorods calcined at 300 °C, (C) β-FeOOH nanorods reduced with N_2H_4 at 80 °C; and (D-F) the corresponding HRTEM images with labeled lattice spacing and crystal planes. Reprinted with permission from (Yue et al., 2011).

3.1 Co-precipitation

One simple and efficient way is to use co-precipitation technique in solution. By this approach, iron(II) and/or iron(III) salts are first dissolved in aqueous solution, and then one alkaline media (e.g., NaOH, Na_2CO_3) solution is added to form precipitate. The prepared particles can be tuned to be uniform in size, shape as well as pure in its composition. Various crystalline phases of iron oxides can be produced using this method, which is controlled by experimental parameters such as types of iron salts (e.g., chloride, sulphate and nitrate), alkaline media, concentration, temperature, and pH (Iida et al., 2007).

Moreover, the phase of iron oxide(s) formed through the co-precipitate approach is often reported as goethite or hematite if iron(III) salt is used. However, the initially precipitated material is usually found as ferrihydrite, which is a thermodynamically unstable phase. The precipitate can further convert into other phases (e.g., hematite, magnetite) depending on the pH, ionic medium, and temperature. For example, Varada et al. (2002) prepared monodispersed acicular goethite particles by precipitating Fe(III) using sodium carbonate. If sodium hydroxide was used, the axial ratio of particles will increase from 60 to 230 nm. It was proposed that different bases have different ability to maintain the solution at a constant pH, where other pH levels would produce polydispersed and hematite particles. The mechanism of the growth of spherical hematite nanoparticles has been explored by Liu et al.(2007). The variation in the final pH of the solution plays a key role in the formation of hematite at different sizes. They found that the particles with diameter of 60-80 nm were obtained at pH 7, while reduced to 30-40 nm in diameter at pH 9.

Synthesis media	Synthesis methods	Common products	Particle shape/size	Features	References
Solid state	Mechanical milling	δ-Fe_2O_3, Fe_3O_4	Spheres D= 2.9-3.6 nm	Mechanical energy to smash.	Lu et al. (2007)
Liquid state	Co-precipitation	α-Fe_2O_3, δ-Fe_2O_3, Fe_3O_4	Nanospheres (d = 30 - 80 nm)	Ageing of ferric and ferrous salts in a basic medium.	Liu et al. (2007)
	Hydrothermal	α-Fe_2O_3, δ-Fe_2O_3, Fe_3O_4 (α-FeOOH β-FeOOH	Nanorods (l: 400-600 nm, w =20-30 nm) Nanodiscs (d = 50 nm, thickness = 6.5 nm)	Low temperature, reaction, commonly conducted in autoclaves, and high efficiency.	Li et al. (2006); Yue et al. (2010, 2011); Jiang et al. (2009)
	Thermal decomposition	α-Fe_2O_3, δ-Fe_2O_3, Fe_3O_4	Nanospheres (d = 16 nm)	High-temperature decomposition of iron organic precursors.	Sun et al. (2004)
	Sol-gel	α-Fe_2O_3, δ-Fe_2O_3, Fe_3O_4	Nanoparticles (24-52 nm)	Dissolve, condensation, and calcinations of alkoxides.	Dong and Zhu (2004)
	Microemulsion	α-Fe_2O_3, δ-Fe_2O_3, Fe_3O_4	Nanoparticles (3-5 nm)	Reaction in two immiscible phases (water and oil).	Vidal-Vidal et al. (2006)
	Sonochemical	Fe_2O_3, Fe_3O_4	Nanorods 10-80 nm in diameter	Ultrasound to promote chemical reaction.	Vijayakumar et al. (2000, 2001)
	Electrochemical	γ-Fe_2O_3	Nanoparticles (d= 3-20 nm)	Electrons act as reactant with no pollution.	Zhang et al (2007); Pascal et al (1999)
Gas state	Spray pyrolysis	δ-Fe_2O_3, Fe_3O_4	Hollow nanospheres, (d =300 nm)	Spraying, aerosol evaporation, condensation, drying, and thermolysis.	González-Carreño et al. (1993)
	Laser pyrolysis or deposition	α-Fe_2O_3, δ-Fe_2O_3, ε-Fe_2O_3 Fe_3O_4	Nanowires (30 nm ×1-5 μm) Nanobelts (100 nm × 7 μm)	Heating of a gaseous mixture of iron precursor.	Morber et al. (2006)

Table 2. Several typical synthesis methods for iron oxides

3.2 Hydrothermal and thermal decomposition methods

Hydrothermal technique is defined as any heterogeneous reaction in the presence of aqueous solvents or mineralizers under a high pressure and a temperature (6-10 atm, 100-200 °C). A hydrothermal reaction requires the iron(III) salt (e.g., iron chloride, nitrate, or sulphate), which can be dissolved in solution followed by reaction with water. This is different from the thermal decomposition reaction that generally takes place for those iron organic precursors ($Fe(CO)_5$, $Fe(acac)_3$, and $Fe(cup)_3$)in an organic solvent at high temperatures (Hyeon et al., 2001; Li et al., 2004; Rockenberger et al., 1999). Both hydrothermal and thermal decomposition methods are commonly used for the synthesis of iron oxide nanoparticles.

The hydrothermal method is often performed in an autoclave, where the reaction system can exceed the boiling point of liquid(s) at normal atmospheric pressure (Jia et al., 2005). The temperature can alter the system in such a way that disrupts the thermodynamics of a material, which is governed by enthalpy (ΔH) and entropy (ΔS), and hence Gibbs free energy (ΔG). The essential role of a fluid under high temperatures is that it changes the vapor pressure of the fluid. This is also beneficial for diverse choices of solvents (polar and non-polar). The morphology and crystalline phase of iron oxides produced through this approach can vary by simply tuning reaction temperature, concentration, and additive(s) (Almeida et al., 2009; Jiang et al., 2010).

The synthesis of iron oxide nanoparticles via a hydrothermal approach can be conducted with or without the use of surfactant(s). Hematite nanoparticles have been prepared by Sahu et al. (1997) under conditions of pH (3-10) and 180 °C in autoclaves. In this study, the average particle size of hematite nanoparticles was found to decrease with an increase of pH. In our recent work (Jiang et al. 2010), we reported a facile hydrothermal route for the synthesis of monodispersed hematite nanodiscs with diameters of ~ 50 nm and thickness of ~6.5 nm in the absence of any surfactants in water at around 90 °C (**Fig. 2**). The nanodiscs exhibited interesting paramagnetic property at a low temperature (20 K), but ferromagnetic at room temperature (~300 K). In addition, the hematite nanodiscs also showed low-temperature catalytic activity in CO oxidation to CO_2.

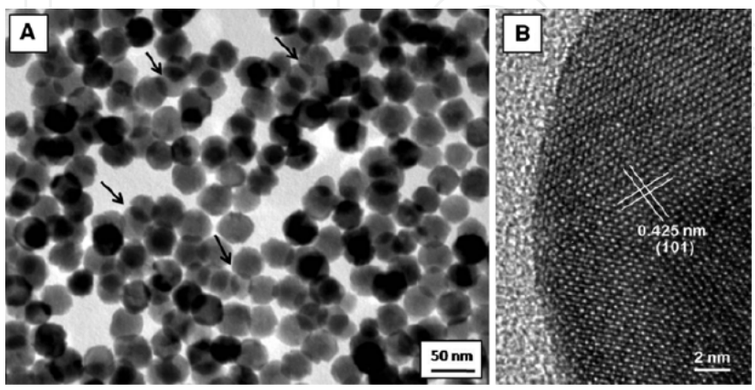

Fig. 2. A) TEM image of α-Fe_2O_3 nanodiscs with overlapping as pointed by arrows; B) HRTEM image showing the lattice fringe of {110} plates with spacing between two adjacent planes of 0.411 nm. Reprinted with permission from (Jiang et al. 2010).

3.3 Microemulsion

Microemulsion method (surfactant-stabilized water/oil (W/O) microemulsion) has been widely used to prepare shape- and size-controlled iron oxide nanoparticles. Generally, a microemulsion is transparent, isotropic and thermodynamically stable dispersion of two immiscible phases (e.g., water and oil). When a surfactant is present in W/O system, the surfactant molecules may form a monolayer at the interface of oil and water, with the hydrophobic tails of the surfactant molecules dissolved in the oil phase and the hydrophilic head groups in the aqueous phase (Wu et al., 2008). In a binary system such as water/surfactant or oil/surfactant, a variety of self-assembled structures can be formed, ranging from spherical and cylindrical micelles to lamellar phases or bi-continuous microemulsions depending on the molar ratio of water, oil and surfactant(s). This will be useful for the generation of nanoparticles with different shapes and sizes.

For example, magnetite nanoparticles ~4 nm in diameter have been prepared by the controlled hydrolysis of ammonium hydroxide with $FeCl_2$ and $FeCl_3$ aqueous solution within the reverse micelles nanocavities generated by sodium bis(2-ethylhexyl) sulfosuccinate (AOT) as a surfactant and heptane as a continuous oil phase (López-Quintela and Rivas, 1993). Lee and co-workers (2005) have successfully synthesized uniform and highly crystalline magnetite nanoparticles in microemulsion nanoreactors. The particle size of the prepared magnetite nanoparticles could be adjusted from 2-10 nm by varying the relative concentrations of iron salt, surfactant, and solvent. Li et al (2009) demonstrated the effect of volumetric ratios of aqueous $FeCl_3$ solution to 1,2-propanediamine on the formation of magnetic particles, as shown in **Fig. 3**. Chin and Yaacob (2007) reported the synthesis of

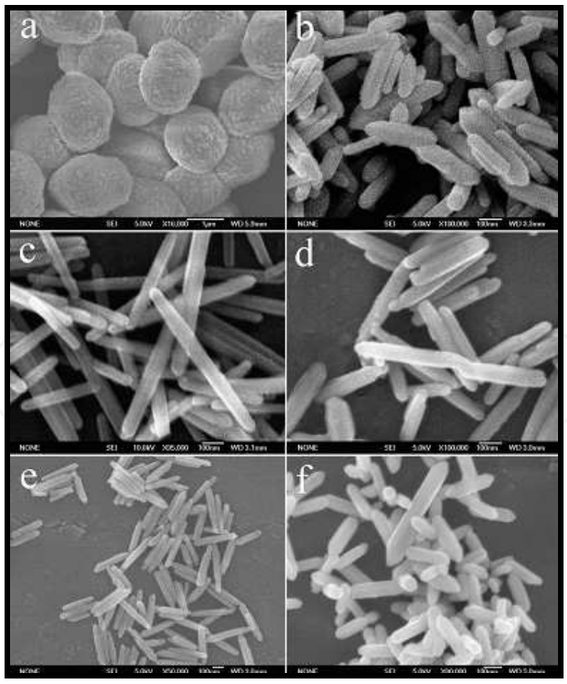

Fig. 3. SEM images of the products obtained at different volume ratios of aqueous $FeCl_3$ solution to 1,2 propanediamine: (a) without 1,2 propanediamine, (b) 3:1, (c) 1:1, (d) 1:2, (e) 1:4, and (f) 1:5. Reprinted with permission from (Li et al., 2009).

magnetic iron oxide nanoparticles with an average particle size of <10 nm by mixing two microemulsion systems, one containing Fe^{2+} ions and the other containing OH^- ions. The study reveals that the nanoparticles prepared by the microemulsion technique were smaller in size and higher in saturation magnetization than those nanoparticles prepared by Massart's procedure (Massart et al., 1981).

Despite some success, this microemulsion approach has some drawbacks, such as the difficulty in scale-up production, the adverse effect of residual surfactants on the properties of the nanoparticles, and the aggregation of the produced nanoparticles. Repeated wash processes and further stabilization treatment are usually required for such a reaction approach (Wu et al., 2008).

4. Surface modifications

The surface modifications of nanoparticles have attracted much more attention, which can improve the surface-related properties like hydrophobic or hydrophilic. This can be achieved by using surfactants, polymers, and inorganic materials (silica).

4.1 Surfactants

Surface modification with surfactant(s) is widely used for altering surface properties such as hydrophobic or hydrophilic. The use of surfactant molecules, such as oleic acid, oleylamine, or thiols (Wang et al., 2005), can easily functionalize iron oxide nanoparticles to be hydrophobic surfaces. These molecules can covalently bond to the iron atoms or clusters against particle degradation (Soler et al., 2007).

Many researches focus on the synthesis of water-soluble iron oxide nanoparticles with biocompatibility and biodegradability for biological applications. For example, one is to directly introduce the biocompatible organic molecules, e.g., amino acid (Sousa et al., 2001), vitamin (Mornet et al., 2004), and citric acid (Morais et al., 2003). Despite some advantages, the instability of small organic molecules in alkaline or acidic environment may result in agglomeration of the functionalized iron oxide nanoparticles.

Another alternative technique is to transform the oil-soluble type into water-soluble one via a ligand exchange reaction (Chen et al., 2008). The ligand exchange involves the addition of an excess of ligand(s) to nanoparticle suspension, which has stronger interaction with the nanoparticles than the original ones. Sun et al. (2003) converted the synthesized hydrophobic maghemite nanoparticles into hydrophilic ones by mixing with bipolar surfactants such as tetramethylammonium 11-aminoudecanoate. Lattuada and Hatton (2006) reported that the oleic groups initially present on the surface of magnetite nanoparticles were replaced by various capping agents containing reactive hydroxyl moieties. They also tuned the particle size in the range of 6-11 nm by varying the heating rate.

4.2 Polymers

Polymer-functionalized iron oxide nanoparticles have gained much more attention due to the benefits offered by polymeric coating, which may increase repulsive forces to balance the magnetic and van der Waals attractive forces acting on the nanoparticles (Wu et al.

2008). It has shown that through careful choice of the passivating and activating polymers and/or reaction conditions, polymer-stabilized iron oxide nanoparticles with tailored and desired properties can be synthesized.

The iron oxide particles by ionic properties can be modified with functional polymer groups with –COOH, $–NH_2$ (Chibowski et al., 2009; Kandori et al., 2005; Li et al., 2004). The polymer coated particles can be synthesized by the *ex situ* method, i.e. dispersion of the nanoparticles in a polymeric solution, or *in situ* method, i.e. monomer polymerization in the presence of the synthesized nanoparticles (Mammeri et al., 2005; Guo et al., 2007).

Polymeric coating materials can be classified into two main classes: natural (e.g., dextran, starch, gelatin, chitosan) and synthetic (e.g., polyethylene glycol, PEG; polymethylmethacrylate, PMMA; polyacrylic acid, PAA). However, the saturation magnetization value of iron oxide nanoparticles will decrease after polymer-fictionalization.

Dextran is often utilized as a coating polymer because of its stability and biocompatibility (Laurent et al. 2008). Molday and Mackenzie (Molday and Mackenzie, 1982) have reported the formation of Fe_3O_4 in the presence of dextran with molecular weight (MW) of 40,000. In the synthesis of dextran-coated ultra-small superparamagnetic iron oxides (USPIO), the reduction of the terminal glucose of dextran was found to be significant for controlling particle size, stability, and magnetic properties. For low molecular weight dextrans (MW, <10,000), it is difficult to obtain nanoparticles with a small size of <20 nm.

Polyvinyl alcohol (PVA) is a hydrophilic and biocompatible polymer that can be used for particle surface modification to prevent particle agglomeration (Laurent et al. 2008). Lee et al. (1996) have modified the surface of magnetite nanoparticles with PVA by precipitation of iron salts at a high pH (13.8) to form stable magnetite colloidal dispersions, and particle size is around 4 nm. The investigators noted that the crystallinity of the magnetite nanoparticles decreased with PVA concentration increasing, although morphology and particle sizes remained. When PVA is introduced, it reacts with the surface through hydrogen bonding between polar functional groups of the polymer and hydroxylated and/or protonated surface of the iron oxide. In addition to the polymer-surface interactions, PVA is known for its hydrogen bonding interaction, resulting in hydrogel structure embedding the nanoparticles. When the PVA concentration is over the critical saturation value, agglomeration may occur for PVA-coated particles via bridging interactions.

4.3 Polymerized amorphous silica

Polymerized tetraethoxysilane (TEOS) network is often used as a surface coating material for iron oxide nanoparticles as this coating can prevent aggregation in solution, improve the chemical stability, and provide better protection against toxicity (Laurent et al. 2008). Additionally, polymerized silica-coated iron oxide nanoparticles exhibited good biocompatibility and solubility in water. Silica coating can stabilize the magnetite nanoparticles in two different ways: one is by shielding the magnetic dipole interaction with the silica shell, and another one is by enhancing the coulomb repulsion of the magnetic nanoparticles. Such a silica coating increases the size of the particles and decreases the saturation magnetization value.

A commonly used method to coat iron oxide nanoparticles with silica is the well-known Stőber method, in which silica is formed *in situ* via hydrolysis and condensation of a sol-gel precursor such as TEOS. For example, Im et al.(2005) have reported the synthesis of silica colloids loaded with superparamagnetic iron oxide nanoparticles, which revealed that the final size of silica colloids depended upon the concentration of iron oxide nanoparticles because the size of silica was closely related to the number of seeds (emulsion drops). The lower concentration the iron oxide nanoparticles in alcohol, the larger size the obtained colloids.

Another one is aerosol-pyrolysis method, in which silica-coated magnetic nanoparticles were prepared by pyrolysis of a mixed precursor of silicon alkoxides and metal compound in a flame environment (Deng et al. 2005). Tartaj *et al.*(2001) synthesized silica-coated γ-Fe_2O_3 hollow spheres with size of 150 ± 100 nm by aerosol pyrolysis of methanol solution containing iron ammonium citrate and silicon ethoxide.

4.4 Metals

Noble metals (e.g., Au, Ag, Pt, and Pd), possessing unique electronic and catalytic properties, can be utilized to improve the physicochemical properties of magnetic nanoparticles and applications in biomedicine. The coating of iron oxide nanoparticles with noble metals can be helpful to improve stability from aggregation, however, decrease the saturation magnetization value in some cases (Wu et al. 2008).

Several procedures have been employed to synthesize such core-shell nanostructures. For example, Mikhaylova *et al.* (2004) have prepared gold-coated superparamagnetic iron oxide nanoparticles (SPION) using a reverse micelle method. In their study, the reverse micelles were formed from surfactant, cetyltrimethylammonium bromide (CTAB), octane (the oil phase), butanol (the co-surfactant), and an aqueous mixture of $FeCl_3$, $FeCl_2$ and $HAuCl_4$ solutions. They found that the Au-coated SPION retained the superparamagnetic properties for a longer period than those of starch-coated and multi-arm polyethylene glycol (MPEG)-coated ones. Wang et al.(2005) obtained gold coated iron oxide nanoparticles, in which the pre-synthesized Fe_3O_4 nanoparticles were used as seeds during the reduction of gold precursor, $Au(OOCCH_3)_3$. The average size of Fe_3O_4 nanoparticles increases from 5.2 ± 0.5 nm to 6.7 ± 0.7 nm after coating with gold (**Fig. 4**). Fe_3O_4/Au and Fe_3O_4/Au/Ag core/shell nanoparticles with tuneable plasmonic and magnetic properties have been developed by controlling the coating thickness and materials (Xu et al. 2007).

A facile and one-pot synthesis approach has been developed by Zhang et al. (Zhang et al., 2010) for generating metal (Au, Pt, Ag and Au-Pt)/Fe_2O_3 nanocomposites assisted by lysine. Lysine, containing functional groups -NH_2 and –COOH, acts as both a linking molecule to the Fe_2O_3 matrix and a capping agent to stabilize the noble metal nanoparticles for a good dispersion. Jiang et al. (Jiang and Yu, 2009) have demonstrated a facile synthetic method for the preparation of Pd/α-Fe_2O_3 nanocomposites by adding citric acid into a mixture of iron oxide nanoparticles and palladium precursor, $Pd(CH_3CN)_2Cl_2$) under a reflux heating at 90°C for 2 hours. The synthesized Pd/α-Fe_2O_3 nanocomposites inherited the rod-like morphology of the α-Fe_2O_3 nanoparticles and they exhibited superior catalytic activity in CO oxidation compared with pure α-Fe_2O_3 nanoparticles. UV-vis measurement of the nanocomposites revealed the presence of two plasma bands centered at around 383 and 552 nm, which can be assigned to the synergistic effect of both Pd and α-Fe_2O_3 nanoparticles.

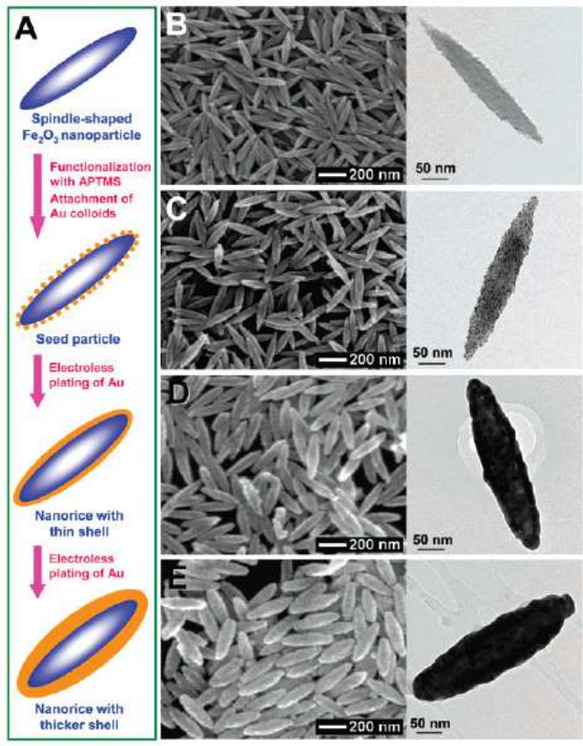

Fig. 4. (A) Schematics of the hematite-gold core-shell nanorice particles. SEM (left) and TEM (right) of (B) hematite core, (C) seed particles, (D) nanorice with thin shells, and (E) nanorice with thick shells. Reprinted with permission from (Wang et al., 2006).

4.5 Carbon

Carbon has been widely studied since its poly-morphologies as active carbon, graphite, graphene, carbon nanotubes, and fullerene bucky ball structures. They have exhibited extraordinary tensile strengths and electrical conductivity due to their covalent *sp*2 hybridized network structure. The combination of semi-conductive iron oxides and carbon may therefore enhance the electrical properties of the nanocomposite material. The method to coat carbon on the surface of iron oxide is often performed by the decomposition of a carbon source (i.e., hydrocarbons, polymer or glucose) at high temperatures under oxygen-free environments (Tristão et al., 2010; Tristão et al., 2009; Zhang et al., 2008, 2010).

Carbon coated iron oxide particles have attracted much more attention. Zhang et al. (2008) demonstrated that carbon coated magnetite nanorods can be synthesized through a series of procedures. In this process, hematite nanorods were firstly synthesized by a hydrothermal method as previously mentioned. Secondly, glucose was coated onto the hematite nanorods by pyrolysis under hydrothermal conditions. Finally, the product was heated at 600 ^{o}C under N_2 to carbonize glucose and reduce hematite into magnetite simultaneously. Boguslavsky et al.(2008) reported a similar procedure, in which polydivinylbenzene (PDVB) was used as the carbon source. The PDVB coating was formed by emulsion polymerization of DVB in the presence of γ-Fe_2O_3, followed by annealing of the powder in a quartz tube at 1050 ^{o}C under flowing Ar gas for 2 hours. The decomposition of the polymer in this case reduced γ-Fe_2O_3 to metallic Fe, which finally forms carbon coated iron (Fe/C) nanoparticles.

In addition, Wang et al. (2006) have reported the synthesis of Fe_3O_4/C nanocomposites by heating the aqueous solution of glucose and oleic acid-stabilized Fe_3O_4 nanoparticles at 170 °C for 3 hours. The results revealed that without prior surface hydrophobic modification, the magnetite nanoparticles could not be encapsulated by the carbon nanospheres, but instead only bare carbon nanospheres with the size of ~200 nm and Fe_3O_4 nanoparticles were obtained. The variation of glucose concentration (0.3-0.6 M) and the reaction temperature (160-180 °C) were found to have no significant effect on the morphology of the product, however, both reaction time and the amount of oleic acid-stabilized Fe_3O_4 nanoparticles showed significant effects. The increase in the concentration of oleic-acid stabilized Fe_3O_4 nanoparticles from 2.5 to 6 g/L was found to generate a product that has more embedded Fe_3O_4 nanoparticles increasing from 41 to 63%).

Although carbon-coated iron oxide nanoparticles may offer some advantages, such particles are often obtained as agglomerated clusters due to the lack of effective synthetic control, and lack of proper understanding on the formation mechanism. The synthesis of dispersible carbon-coated nanoparticles in isolated forms still remains a challenge in this field.

Moreover, the surface modification of iron oxide allows the attachment of biomolecules such as proteins and drugs (Mohapatra et al. 2007; Sun et al. 2007). The design of the surface modifications may be determined by factors such as ion energy and ion flux of depositing species, interface volume, crystalline size, coating thickness, surface and interfacial energy (Kim et al. 2003; Pinho et al. 2010).

5. Functionalities of iron oxide nanostructures

5.1 Magnetic property

The magnetic property has been extensively studied since it was discovered and explained through electronic structures of atoms. The magnetic dipole moments generated by the spin and orbital angular momenta of electrons in the Fe atom may vary between each phase of the iron oxide material. In general, magnetic behavior of a material depends on the electron spin vector or the total magnetic dipole moment. One important aspect in iron oxide nanoparticles is the unique form of magnetism called superparamagnetism. At temperature of above the blocking temperature, the magnetization behavior is identical to that of atomic paramagnets. This phenomenon will occur if particles reach below a certain size (10-20 nm), when the particle consists of a single magnetic domain, even though the material is ferro- or ferri-magnetic in bulk form (Ye et al., 2007), as shown in **Fig. 5**. Particles with this type of magnetism show high field irreversibility, high saturation field, extra anisotropy contributions, and shifted loops (Pedro et al., 2003).

For noble gold and silver nanoparticles with unique surface plasmon resonance (SPR) properties, they are often used to modify the iron oxide surfaces for generating coupled or multiple functionalities. At the nanoscale, the metallic electron cloud oscillates on the particle surface and absorbs electromagnetic radiation at a particular energy. The surface geometry of the iron oxide particles such as spheres, cubes, triangles, or rods, can therefore influence the absorption of radiation from the ultra-violet up to the near infrared spectrum (350-1200 nm). Other factors that affect the absorption are the solvent and surface functionalization. They are important contributors that can tune the exact frequency and intensity of the plasmon resonance band, which attracts them to the surface enhanced

resonance spectroscopy (SERS) for sensing devices (Zhai et al., 2009). This effect is also of importance for bimetallic core/shell nanoparticles. As the ratio of gold to iron oxide increases, the gold character increases and the iron oxide becomes buried beneath and suppresses the dielectric effect. The increasing thickness of the shell structure will therefore cause blue-shifting in the surface plasmon resonance (Lyon et al. 2004).

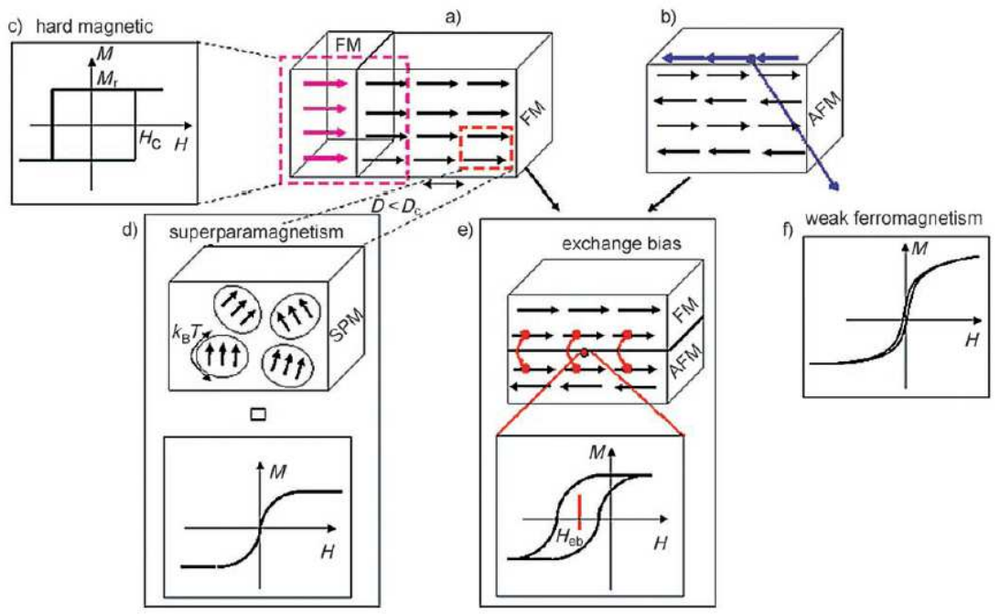

Fig. 5. Diagram of different spin arrangements in magnetic nanoparticles:
a) Ferromagnetism (FM), b) Antiferromagnetism (AFM), D = diameter, D_c = critical diameter, c) a combination of two different ferromagnetic phases in permanent magnets, which are materials with high remanence magnetization (M_r) and high coercively (H_c), d) Superparamagnetism (SPM), e) the interaction at the interface between a ferromagnet and an antiferromagnet producing an exchange bias effect, and f) pure anti-ferromagnetic nanoparticles with superparamagnetic relaxation arising from uncompensated surface spins. Reprinted with permission from (Lu et al., 2007).

5.2 Biomedical applications

Many investigations have been reported the application of nanoparticles for biomedicine, such as magnetic nanoparticles for improving the quality of magnetic resonance imaging (MRI), hyperthermic treatment for malignant cells, site-specific drug delivery, cell labeling, and manipulating cell membranes (Babič et al. 2008; Catherine and Adam, 2003). These magnetic particles can also be used for diagnosis, imaging, and drug delivery.

Iron oxide nanocomposites or particle coated with biocompatible polymer(s) have shown some advantages, e.g., reducing aggregation, maintain magnetic stability, slowdown degrading process under physiological conditions, and lower toxicity (Mahmoudi et al. 2009). So far, they have shown promise for monitoring living cells by both MR and fluorescence imaging, as well as for drug delivery (Liong et al., 2008).

As mentioned previously, iron oxide nanoparticles exhibit paramagnetic or superparamagnetic properties in a limited size range. Particles larger than 50 nm show superparamagnetic iron oxides (SPIO), whereas particles smaller than 50 nm show ultrasmall superparamagnetic property (USP). The smaller ones have the ability to enhance signal detection and increase resolution in the MRI (Foy et al., 2010; Tong et al., 2010). Therefore, the SPIO particles can be used for imaging tumors in the liver and spleen, while superparamagnetic particles for contrast agents for lymphography and angiography. However, the superparamagnetic particles do not retain their magnetism when the external magnetic field is removed, while other magnetic materials will become magnetized and aggregate.

In addition, the problem using magnetite or maghemite nanoparticles in clinic is often limited by the biocompatibility and toxicity of these particles (Martin et al., 2008; Pisanic Ii et al., 2007). This happens from the body's defense system, the reticulo-endothelial system (RES), trying to remove these particles from the bloodstream as they pass through the liver, spleen and lymph nodes. The rapid removal of the iron oxide nanoparticles reduces their life-time. This is why it is necessary to produce nanocomposites with special surface modifications. The surface modification of the particles allows the water-insoluble drugs to be loaded and stored for a long time (Liong et al., 2008; Son et al., 2005). Despite some progress, the challenges in using surface modified magnetic iron oxide nanoparticles still exist. More work needs to be performed in the future.

5.3 Gas sensing

Gas detection with high sensitivity and selectivity is essential for controlling industrial, waste, and vehicle emissions, household activity and environmental monitoring. In the past decades, many sensor devices have been developed for various gases such as CO, CO_2, O_2, O_3, H_2, NH_3 and SO_2, as well as various organic vapors e.g., benzene, methanol, ethanol, amines and isopropanol (Jimenez-Cadena et al. 2007). Although semiconducting oxides have been quite useful as gas sensors, the operation at high temperatures often limits their functionality and applications. This has prompted the exploration of new materials that may offer higher sensing and selective capabilities than traditional ones.

Nanostructured metal oxides are one of the most commonly used materials for gas sensing because of the semiconductors make them possible for the electrical conductivity change when the surrounding atmosphere changes. Additionally, nanosized metal oxides exhibit high ratios of surface to volume, which favors the adsorption of gases on the particle surface, and hence increases the sensitivity in detection.

Iron oxide nanoparticles have shown good sensing capabilities toward hydrocarbon gases, CO and alcohols (Jimenez-Cadena et al., 2007; Han et al., 1996, 1999, and 2001). The studies by Zhang et al. (1996) and Tao et al. (1999) showed that γ-Fe_2O_3 nanosensors exhibited good sensitivity and selectivity to a range of hydrocarbon gases such as LPG, petrol and C_2H_2 at 380 °C, but poor sensitivity to H_2 and CO. However, Nakatani and Matsuoka (1983) together with Lee and Choi (1990) reported that the γ-Fe_2O_3-based sensors exhibited good sensitivity to H_2. This suggests that the gas-sensing characteristics of a nanosensor are related to its preparation process.

The sensitivity of iron oxide-based nanosensors can be improved by various doping schemes as well as by changing the sensing material structure. For example, the thin film type sensors tend to exhibit higher sensitivity than bulk material sensor(s) (Mohapatra and Anand, 2010). Tao and co-workers (1999) have studied the sensing characteristics of Y_2O_3-doped γ-Fe_2O_3 towards hydrocarbon gases, H_2 and CO and found that the addition of Y_2O_3 to γ-Fe_2O_3 resulted in a little difference in the sensitivity and selectivity compared with those made of pure γ-Fe_2O_3. Neri et al.(2002) have assessed the gas-sensing properties of Zn-doped Fe_2O_3 thin films prepared by liquid phase deposition method. They observed that the addition of metal Zn can increase the sensitivity of the Fe_2O_3 thin film to NO_2 below 250 °C.

5.4 Catalyst

A catalyst can attract atoms and/or molecules, and then change the surface conductivity and other properties. Different from sensing material, the catalyst often converts itself into a different species through a chemical reaction. The iron oxides (hematite and magnetite) have been applied in industry to produce chemicals with high efficiencies, such as ammonia (Haber process) and hydrocarbons (Fischer-Tropsch process) (Teja and Koh, 2009). It is expected that the nanoparticles with high surface areas can perform much better to enhance the chemical reaction rates than that of bulk states. For hematite, its thermal-dynamically stable structure allows it for high temperature oxidation catalysis (Sivula et al., 2010).

The catalysis effect can also be enhanced by coupling metal nanoparticles on the surface (Jiang and Yu 2009; Zhong et al., 2007). Jiang et al (2009) have reported the synthesis of Pd/α-Fe_2O_3 nanocomposites at ambient conditions, which displayed superior low-temperature catalytic activity toward CO oxidation to the pure α-Fe_2O_3 nanoparticles. It was proposed that the enhanced catalytic activity was due to the reaction between oxygen adsorbed on the reduced sites of the support (Fe^{2+}) and CO adsorbed on Pd at the metal-oxide interface, as shown in **Fig. 6**.

By using gold deposited iron oxide materials as a catalyst material, the oxidation and hydrogenation reaction of many organic compounds can be performed at much lower temperatures (Kung et al., 2007; Herzing et al., 2008; Lenz et al., 2009; Scirè et al., 2008). For example, Al-Sayari and co-workers (2007) have shown the dependence of the catalytic performance of Au/Fe_2O_3 catalyst that the non-calcined Au/Fe_2O_3 catalyst exhibited a high activity when pH≥ 5, whereas the activity of calcined Au/Fe_2O_3 catalyst was not influenced by the preparation conditions. Furthermore, the authors also noted that the catalytic activity of Fe_2O_3 toward CO oxidation was considerably lower than that of the Au/Fe_2O_3 catalyst.

Maghemite and magnetite/carbon composites have been found to be good catalysts for reducing the concentration of undesirable nitrogen in acrylonitrile-butadiene-styrene (ABS) degradation oil (Brebu et al., 2001), whereas hematite can be used as a photocatalyst for the degradation of chlorophenol and azo dyes (Bandara et al., 2007), as well as a support material for gold in catalysts for the oxidation of carbon monoxide (CO) at low temperatures (Zhong et al., 2007).

The challenge of catalysis research being the reaction mechanism for these systems are still yet to be confirmed or explained, especially for the metal oxide/gold systems (Astruc et al., 2005). The reaction can be compared from titanium oxide/gold. The rutile phase of titania provides a support for gold, in which CO will convert mostly along the perimeter between the titania and

gold (Haruta, 2002). In other studies, it was proposed that the nature of the support material has much greater influence on the reactive properties of the deposited nanoparticle, because the active and selective sites are formed by negative gold particles (Milone et al., 2007).

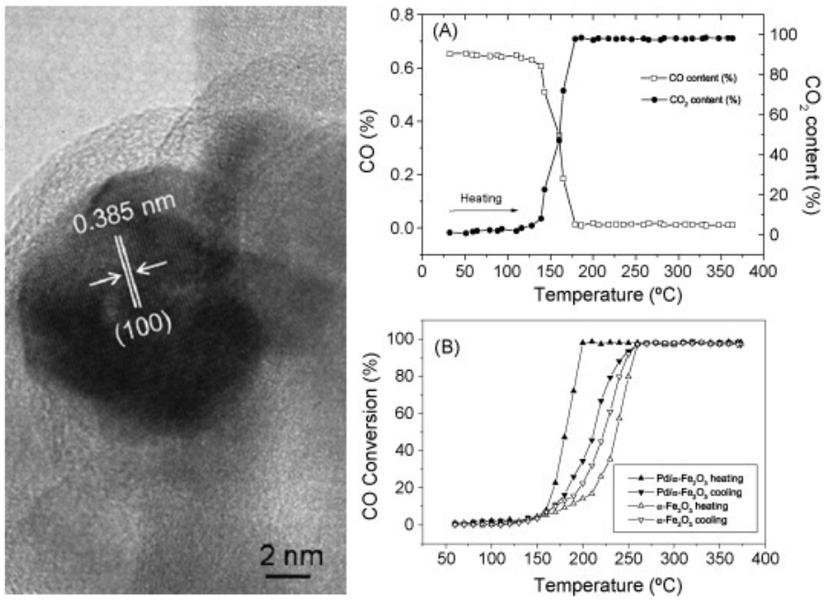

Fig. 6. HRTEM image of Pd particles binding on the surface of iron oxide, in which the lattice distance is ~0.385 nm, corresponding to Pd{1 0 0} planes. Catalytic activity of Pd/α-Fe_2O_3 nanocomposites showing the dependence of CO oxidation (A); (B) comparison of the catalytic activity of nanoparticles with and without doped palladium. Reprinted with permission from (Jiang and Yu, 2009).

6. Theoretical simulations

Beyond physical phenomena, theoretical methods have been developed and widely used to understand electronic, structure and forces of nanostructures (Cohen et al., 2008; Freund and Pacchioni, 2008; Hafner et al., 2006; Carter, 2008). Specifically, molecular dynamics (MD) method can be used for calculating interaction energies between surface modifiers and the modified matters, density functional theory (DFT) for binding energies, and Monte Carlo (MC) method for equilibrium properties (e.g., free energy, phase equilibrium) of particles. These methods have allowed researchers to understand and explain the growth mechanisms, structure, and functionalities of nanostructures (Hafner et al., 2006).

6.1 Molecular dynamics

MD simulation has been widely used for the study of the molecular behaviours in liquids and solids, examining material properties, and designing new materials, particularly for nanoparticles and nanocomposites. The MD method allows one to predict the time evolution of a system of interacting particles (atoms or molecules) and estimate relevant physicochemical properties. Specifically, it can calculate and simulate the interaction energies among atoms/molecules, which can help understand atomic positions, velocities,

and forces. Thus, the macroscopic properties (e.g., pressure, energy, heat capacities) can be derived by means of statistical mechanics.

In our recent work, the MD method was used to explain the interactions between various goethite surfaces and surfactants of the nanorods. The simulation results of the side wall (*xy*0) surfaces with six different surfactants have been reported (Yue et al. 2010, 2011). The positively charged surfactants, CTAB (**Fig. 7**) and tetraethylammonium chloride (TEAC), were found to interact greatly with the side wall (*xy*0) of the nanorod, while the polymeric polyethylene glycol (PEG) and polyvinylpyrrolidone (PVP) and anionic surfactants (AOT) and Sodium Dodecyl Sulfate (SDS) were not suitable because of the low interaction energies among the surfaces. This is caused by the differences in the active sites on different surfaces (Kim et al. 2007). The ratios of iron and oxygen can vary greatly for different surfaces, in which the packing and exposure of atoms along a particular crystal plane will therefore determine the strength of adsorbed surface molecules. The simulation could provide quantitative information toward the interaction between surfactants and goethite surface(s), and hence understand the particle formation and growth mechanisms.

Through a similar MD simulation, the adsorption of minerals has been explored. Kerisit et al. (2006) simulated the interactions for electrolyte solutions to determine the surface properties of monovalent ions, such as NaCl, CsCl, and CsF on the (100) goethite surface. The calculations showed a structured interfacial region is in the first 15 Å on the surface. The structure of the mineral surface will also affect the arrangement and orientation of the water molecules, and hence the diffusive properties and distribution of the ionic species. In comparison, the adsorption of sodium ions is stronger than cesium ions because the former can occupy an interstitial site of mineral(s) due to smaller size.

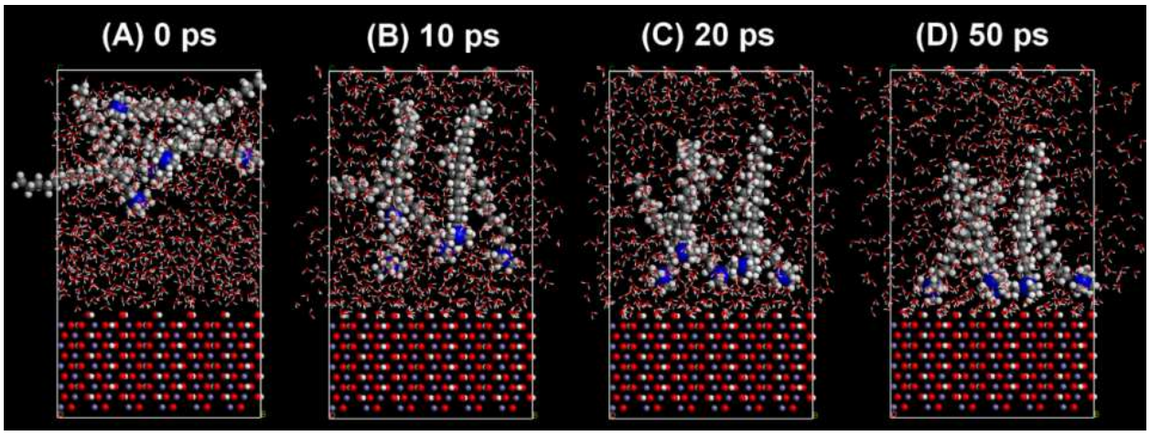

Fig. 7. MD simulation of CTAB molecular adsorption on the goethite crystal (010) surface at different time: (A) 0 ps, (B) 10 ps, (C) 20 ps, and (D) 50 ps. Reprinted with permission from (Yue et al., 2010).

Similarly, MD simulation was also employed to explain the growth mechanisms of akaganéite nanorods (Yue et al., 2011), as shown in **Fig. 8**, in which the atomic concentration profiles of various anions on different crystalline surfaces were compared. With the assistance of experimental techniques such as transmission electron microscopy (TEM), energy dispersive spectroscopy (EDS), and x-ray diffraction (XRD), the role of chloride ions in the lattice

structure and forming β-FeOOH rodlike structure was determined. The analysis showed that the chloride ions were a small size, as well as having an intermediate interaction on the tunnel structure of the (001) surface, while the tight packing of the (100) and (110) surfaces does not allow interaction with any ions. The information was useful for the development of the simulation model, which explained the filling of the tunnel structure along (001) direction.

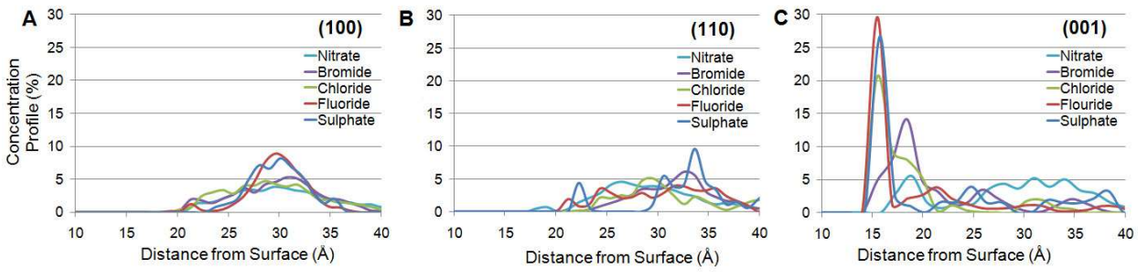

Fig. 8. The concentration profiles of various anions on the crystal surface of akaganéite nanorods: (A) (100); (B) (110); and (C) (001) plane.
Reprinted with permission from (Yue et al., 2011).

This MD method is used not only for small organic molecules but also for metallic nanoclusters. In our recent work (Yue et al., 2011), the Fe_3O_4(111) surface modified with various surfactants, polymers, and silica, followed by the deposition of a Au nanoparticle was simulated by MD method). The results show the dynamic motion of the molecules on the Fe_3O_4(111) surface, followed by the encapsulation of the Au nanoparticle surface. Through an analysis of the concentration profile, it reveals that $–NH_2$ groups within the molecule(s) are useful for attracting gold atoms, as shown in **Fig. 9**. Moreover, one-dimensional chainlike molecules allow higher flexibility to move toward the Au surface compared with three-dimensional structure (amorphous or polymerized silica)

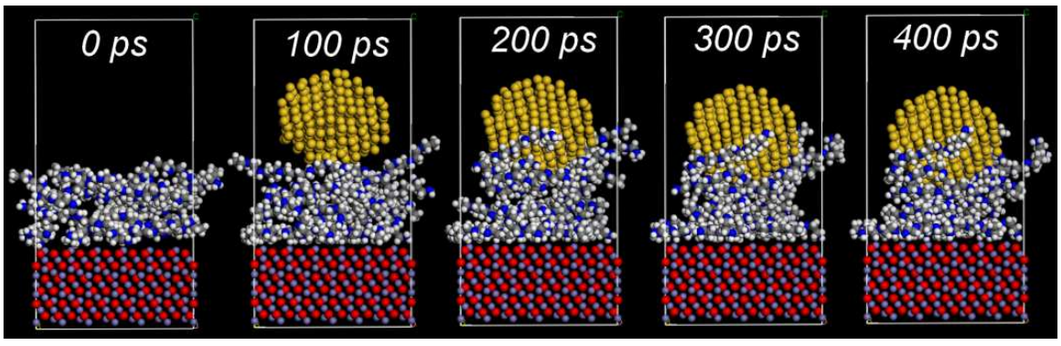

Fig. 9. Snapshots of PEI coating onto the surface of Fe_3O_4(111) and the addition of a AuNP at various times. Reprinted with permission from (Yue et al., 2011).

This theoretical method is available for predicting the interaction energies and adsorption sites of molecules on the iron oxides surfaces. Aquino et al.(2006) simulated various molecules such as water, acetic acid, acetate, 2,4-dichlorophenoxyacetic acid, and benzene on the goethite (110) surface. The results show that two OH types, hydroxo and μ-hydroxo, were able to bend and act as proton acceptors, while the third type, μ_3-hydroxo, acts only as proton donor due to its more pronounced rigidity.

However, MD is a classical simulation method which uses parameterized potentials (or forcefields), which cannot quantify electronic information of nanostructures. This method is limited to its accuracy, although the results can be obtained within a realistic period of time and larger length scales (Rustad et al., 2003; Zeng et al., 2008).

6.2 Density functional theory

DFT is another powerful simulation technique for understanding atom/molecular binder energies. The calculation is performed by using approximation method to simplify the Schrödinger's equation (Lado-Touriño and Tsobnang, 2000).

Many DFT studies have emphasized on the structural, electronic, catalytic, and magnetic properties of metal-oxide, such as Fe_2O_3, and Al_2O_3 (Alvarez-Ramirez et al., 2004; Ma et al., 2006; Mason et al., 2009; Rohrbach et al., 2004; Rollmann et al., 2004; Zhong et al., 2008; Mason et al., 2010). It has been extended into other systems, e.g., carbon nanotubes or graphene (Li et al., 2010; Chattaraj et al., 2009), transition metals (Cramer et al., 2009), semiconductors (Jin et al., 2011), and metals (e.g., Pd, Au, Cu) (Yang et al., 2007).

For example, Wong et al.(2011) demonstrated that the electronic and geometric structure of different metald (M = Au, Pt, Pd, or Ru) bilayers particularly on the α-Fe_2O_3(0001) support surface (**Fig. 10**). The analysis shows that the synergistic effect depends on the localized electron gain, electron transfer from Fe atoms to the dz^2 orbital of the metal bilayer, and interfacial metallic/ionic bonding. These effects were most pronounced for surfaces modified with Pt or Ru, while the Au bilayer is the most stable due to its low α-Fe_2O_3 lattice deformation and minimal surface of Fe atom spin quenching. Tuning the Ru bilayer can provide an optimal balance of these factors, and hence enhance the catalytic activity.

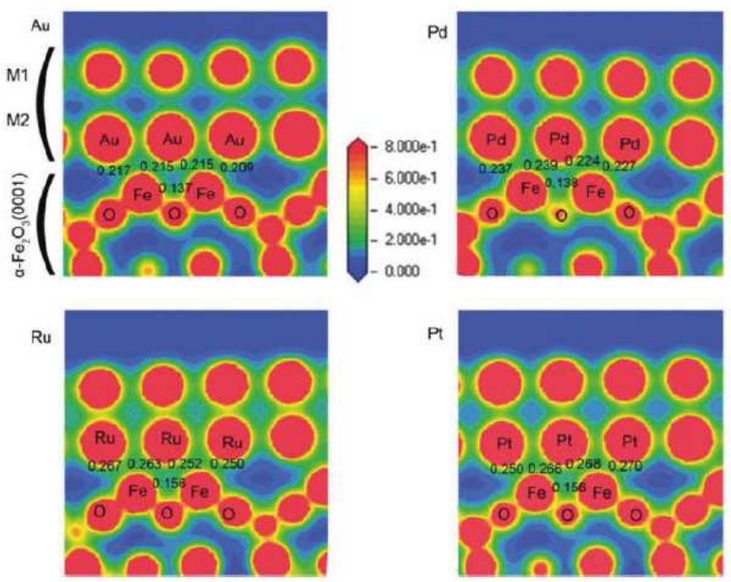

Fig. 10. Electron density contour maps of M/α-Fe_2O_3(0001) interfaces, where M = Ru, Pd, Au, and Pt, respectively, and the electron density is in the range 0.0−0.8 eV/Å^3. Reprinted with permission from (Wong et al., 2011).

Despite some success, the DFT method still has limitations in accurately describing the van der Waals interactions, phonon dispersion, spin-and space-degenerate states, strongly conjugated π systems, localization and delocalization errors for band gaps. Moreover, the DFT is difficult to solve the problems related to long range interactions and dispersion forces for complex biological systems. So far, the development of DFT technique is still demanded.

Besides DFT and MD simulations, Monte Carlo (MC) method, a stochastic method, has been employed to generate a statistical or probabilistic model for understanding particular systems. The MC method can be used to predict the crystalline structure of β-FeOOH (Kwon et al. 2006). By combination of quantitative X-ray structural analysis, the MC simulation has been used for characterizing the atomic-scale structure with and without chromium atoms. The results showed that the β-FeOOH particles containing chromium is distorted, while the particles without chromium is similar to its ideal structure. The combination of the experimental and MC simulation method can distinguish the differences between FeO_6 and CrO_6 octahedral units. However, this MC method can only provide information on equilibrium properties (e.g., free energy, phase equilibrium), but limited to the non-equilibrium systems.

7. Summary

This Chapter briefly overviews some experimental methods (hydrothermal, co-precipitate and microemulsion methods) used for the synthesis and surface modifications of low-dimensional iron oxide nanostructures with desirable functional properties (gas sensing, catalytic, magnetic, and biochemical properties), and a few theoretical simulation techniques (MD, DFT, and MC) for fundamental understandings. However, the challenges still exist. Experimentally, one of the big challenges is how to produce iron oxide nanostructures with desired characteristics (shape, size, and surface properties) for target applications. Theoretically, DFT and MD simulations are limited to the large-scale calculations (e.g., mesoscopic structure with size range of 0.1–10 μm) due to the current restraints in computational capability.

To overcome the limitations, the development of simple, cost-saving, and effective strategies for iron oxide and other nanostructures with desirable functional properties is highly demanded. For the computational modelings and simulation methods, much work needs to be performed in two directions: (i) to develop new and improved simulation techniques for large time and length scales; and (ii) to integrate diverse simulation techniques (DFT, MD, MC and others) on different levels together to form a powerful tool for exploring the structural, dynamic, and mechanical properties of nanomaterials and nanosystems. This is crucial to predict process–structure–property relationships in material design, optimization, and manufacturing.

8. Acknowledgement

We gratefully acknowledge the financial support of the Australia Research Council (ARC) the ARC Centres of Excellence for Functional Nanomaterials and ARC projects. The authors acknowledge access to the UNSW node of the Australian Microscopy & Microanalysis Research Facility (AMMRF).

9. References

Al-Sayari, S., Carley, A.F., Taylor, S.H. & Hutchings, G.J. (2007). Au/ZnO and Au/Fe_2O_3 catalysts for CO oxidation at ambient temperature: comments on the effect of synthesis conditions on the preparation of high activity catalysts prepared by coprecipitation. *Top. Catal.,* 44: 123-128.

Almeida, T.P., Fay, M., Zhu, Y. and Brown, P.D. (2009). Process Map for the Hydrothermal Synthesis of α-Fe_2O_3 Nanorods. *J. Phys. Chem. C,* 113(43): 18689-18698.

Alvarez-Ramirez, F., Martinez-Magadan, J.M., Gomes, J.R.B., & Illas, F. (2004), On the geometric structure of the (0001) hematite surface, *Surface Sci.*, 558, 4-14.

Aquino, A.J.A., Tunega, D., Haberhauer, G., Gerzabek, M.H. and Lischka, H. (2006). Quantum Chemical Adsorption Studies on the (110) Surface of the Mineral Goethite. *J. Phys. Chem. C,* 111(2): 877-885.

Astruc, D., Lu, F. and Aranzaes, J.R. (2005). Nanoparticles as Recyclable Catalysts: The Frontier between Homogeneous and Heterogeneous Catalysis. *Angew. Chem. Int. Ed.,* 44(48): 7852-7872.

Babic, M., Horák, D., Trchová, M., Jendelová, P., Glogarová, K.i., Lesný, P., Herynek, V., Hájek, M. and Syková, E. (2008). Poly(l-lysine)-Modified Iron Oxide Nanoparticles for Stem Cell Labeling. *Bioconjugate Chem.,* 19(3): 740-750.

Bandara, J., Klehm, U. and Kiwi, J. (2007). Raschig rings-Fe_2O_3 composite photocatalyst activate in the degradation of 4-chlorophenol and Orange II under daylight irradiation. *Appl. Catal. B,* 76(1-2): 73-81.

Boguslavsky, Y. & Margel, S. (2008). Synthesis and characterization of poly(divinylbenzene)-coated magnetic iron oxide nanoparticles as precursor for the formation of air-stable carbon-coated iron crystalline nanoparticles. *J. Colloid and Interface Sci.,* 317(1): 101-114.

Bomati-Miguel, O., Rebolledo, A.F. & Tartaj, P. (2008). Controlled formation of porous magnetic nanorods via a liquid/liquid solvothermal method. *Chem. Commun.,* (35): 4168-4170.

Brebu, M., Uddin, M.A., Muto, A., Sakata, Y. & Vasile, C. (2001). Catalytic degradation of acrylonitrile−butadiene−styrene into Fuel Oil 1. The effect of iron oxides on the distribution of nitrogen-containing compounds. *Energy & Fuels,* 15(3): 559-564.

Carter, E.A. (2008). Challenges in modeling materials properties without experimental input. *Science,* 321(5890): 800-803.

Catherine, C.B. & Adam, S.G.C. (2003). Functionalisation of magnetic nanoparticles for applications in biomedicine. *J. Phys. D: Appl. Phys.,* 36(13): R198.

Chattaraj, P.K. (2009). Chemical reactivity theory: a density functional view, pp. 9781420065435.

Chen, Z.P., Zhang, Y., Zhang, S., Xia, J.G., Liu, J.W., Xu, K. & Gu, N. (2008). Preparation and characterization of water-soluble monodisperse magnetic iron oxide nanoparticles via surface double-exchange with DMSA. *Colloids Surf. A,* 316(1-3): 210-216.

Chibowski, S., Patkowski, J. & Grzadka, E. (2009). Adsorption of polyethyleneimine and polymethacrylic acid onto synthesized hematite. *J. Colloid and Interface Sci.,* 329(1): 1-10.

Chin, A.B. and Yaacob, I.I. (2007). Synthesis and characterization of magnetic iron oxide nanoparticles via w/o microemulsion and Massart's procedure. *J. Mater. Process. Tech.,* 191(1-3): 235-237.

Cohen, A.J., Mori-Sánchez, P. & Yang, W. (2008). Insights into current limitations of density functional theory. *Science,* 321(5890): 792-794.

Cornell, R.M., Schuwertmann, U. *The iron oxides: structure, properties, reactions, occurrences, and uses*, Wiley-VCH, Weinheim, 2003.

Cramer, C.J. & Truhlar, D.G. (2009), Density functional theory for transition metals and transition metal chemistry. *Phys. Chem. Chem. Phys*. 11: 10757-10816.

Deng, Y.-H., Wang, C.-C., Hu, J.-H., Yang, W.-L. & Fu, S.-K. (2005). Investigation of formation of silica-coated magnetite nanoparticles via sol-gel approach. *Colloids Surf. A,* 262(1-3): 87-93.

Di Marco, M., Guilbert, I., Port, M., Robic, C., Couvreur, P. and Dubernet, C. (2007). Colloidal stability of ultrasmall superparamagnetic iron oxide (USPIO) particles with different coatings. *Int. J. Pharmaceutics,* 331(2): 197-203, 0378-5173.

Dong, W.T., Zhu, C.S. (2002). Use of Ethylene oxide in the sol–gel synthesis of α-Fe_2O_3 nanoparticles from Fe (III) Salt. *J. Mater. Chem.,* 12 (6): 1676–1683.

Erogbogbo, F., Yong, K.T., Hu, R., Law, W.C., Ding, H., Chang, C.W., Prasad, P.N. & Swihart, M.T. (2010). Biocompatible magnetofluorescent probes: luminescent silicon quantum dots coupled with superparamagnetic iron(III) oxide. *ACS Nano,* 4: 5131-5138.

Foy, S.P., Manthe, R.L., Foy, S.T., Dimitrijevic, S., Krishnamurthy, N. & Labhasetwar, V. (2010). Optical imaging and magnetic field targeting of magnetic nanoparticles in tumors. *ACS Nano,* 4(9): 5217-5224.

Freund, H.-J. & Pacchioni, G. (2008). Oxide ultra-thin films on metals: new materials for the design of supported metal catalysts. *Chem. Soc. Rev.,* 37(10): 2224-2242.

Garcia, K.E., Barrero, C.A, Morales, A.L. & Greneche, J.M. (2009). Magnetic structure of synthetic akaganeite: A review of Mössbauer data. *Rev. Fac. Ing. Univ. Antioquia,* 49*:* 185-191.

González-Carreño, T., Morales M.P., Gracia, M. & Serna, C.J. (1993). Preparation of uniform amma-Fe_2O_3 particles with nanometer size by spray pyrolysis. *Mater. Lett*., 18: 151-155.

Guo, Z., Park, S., Wei, S., Pereira, T., Moldovan, M., BKarki, A., Young, D. P. & Hahn, H. T. (2007). Flexible high-loading particle-reinforced polyurethane magnetic nanocomposite fabrication through particle-surface-initiated polymerization. *Nanotech.* 18: 335704.

Hafner, J., Wolverton, C. & Ceder, G. (2006). Toward computational materials design: the impact of density functional theory on materials research. *MRS Bulletin,* 31: 659-668

Han, J.S., Yu, A.B., He, F.J. & Yao, T (1996). A study of the gas sensitivity of alpha-Fe_2O_3 sensors to CO and CH_4. *J. Mater. Sci. Lett*. 15: 434-436.

Han, J.S., Bredow, T., Davey, D.E., Yu, A.B. & Mulcahy, D.E. (2001). The effect of Al addition on the gas sensing properties of Fe_2O_3-based sensors. *Sens. and Actuators B* 75: 18-23.

Han, J.S., Davey, D.E., Mulcahy, D.E. & Yu, A.B. (1999). An investigation of gas response of alpha-Fe_2O_3(Sn)-based gas sensor. *Sens. and Actuators B* 61: 83-91.

Haruta, M. (2002). Catalysis of gold nanoparticles deposited on metal oxides. *CATTECH,* 6(3): 102-115.

Herzing, A.A., Kiely, C.J., Carley, A.F., Landon, P. & Hutchings, G.J. (2008). Identification of active gold nanoclusters on iron oxide supports for CO oxidation. *Science,* 321(5894): 1331-1335.

Hyeon, T., Lee, S.S., Park, J., Chung, Y. & Na, H.B. (2001). Synthesis of highly crystalline and monodisperse maghemite nanocrystallites without a size-selection Process. *J. Am. Chem. Soc.,* 123(51): 12798-12801.

Iida, H., Takayanagi, K., Nakanishi, T. & Osaka, T. (2007). Synthesis of Fe_3O_4 nanoparticles with various sizes and magnetic properties by controlled hydrolysis. *J. Colloid and Interface Sci.,* 314(1): 274-280.

Ilani, S., Rosenfeld, A. & Dvorachek, M. (1999). Mineralogy and chemistry of a Roman Remedy from Judea, Israel. *J. Archaeological Sci.,* 26(11): 1323-1326.

Im, S.H., Herricks, T., Lee, Y.T. & Xia, Y. (2005). Synthesis and characterization of monodisperse silica colloids loaded with superparamagnetic iron oxide nanoparticles. *Chem. Phys. Lett.,* 401(1-3): 19-23.

Ito, A., Shinkai, M., Honda, H. & Kobayashi, T. (2005). Medical application of functionalized magnetic nanoparticles. *J. Biosci. and Bioeng.,* 100(1): 1-11.

Jia, C.-J., Sun, L.-D., Yan, Z.-G., You, L.-P., Luo, F., Han, X.-D., Pang, Y.-C., Zhang, Z. & Yan, C.-H. (2005). Single-crystalline iron oxide nanotubes. *Angew. Chem. Int. Ed.,* 44(28): 4328-4333.

Jiang, X.C., Yu, A.B., Yang, W.R., Ding, Y., Xu, C. & Lam, S. (2010). Synthesis and growth of hematite nanodiscs through a facile hydrothermal approach. *J. Nanopart. Res.,* 12: 877-893.

Jiang, X.C. &Yu, A.B. (2009). Synthesis of Pd/alpha-Fe_2O_3 nanocomposites for catalytic CO oxidation. *J. Mater. Process. Tech.,* 209(9): 4558-4562.

Jimenez-Cadena, G., Riu, J. & Rius, F.X. (2007). Gas sensors based on nanostructured materials. *Analyst,* 132(11): 1083-1099.

Jin, D., Wang, W., Rahman, A., Lizhen, J., Zhang, H., Li, H., He, P., & Bao, S. (2011), Study on the interface between the organic and inorganic semiconductors, *Appl. Surface Sci.* 257: 4994-4999.

Kandori, K., Yamoto, Y. & Ishikawa, T. (2005). Effects of vinyl series polymers on the formation of hematite particles in a forced hydrolysis reaction. *J. Colloid and Interface Sci.,* 283(2): 432-439.

Kerisit, S., Ilton, E.S. & Parker, S.C. (2006). Molecular Dynamics simulations of electrolyte solutions at the (100) goethite surface. *J. Phys. Chem. B,* 110(41): 20491-20501.

Kim, D.K., Mikhaylova, M., Zhang, Y. & Muhammed, M. (2003). Protective coating of superparamagnetic iron oxide nanoparticles. *Chem. Mater.,* 15(8): 1617-1627.

Kim, H.-G., Kim, D.-W., Oh, C., Park, S.-H. & Oh, S.-G. (2007). Preparation of rod-type ferric oxyhydroxide particles by forced hydrolysis in the presence of a cationic surfactant. *J. Ceramic Process Res.,* 8(3): 172-176.

Kung, M.C., Davis, R.J. & Kung, H.H. (2007). Understanding Au-Catalyzed low-temperature CO oxidation. *J. Phys. Chem. C,* 111(32): 11767-11775.

Kwon, S.K., Suzuki, S., Saito, M., Kamimura, T., Miyuki, H. & Waseda, Y. (2006). Atomic-scale structure of beta-FeOOH containing chromium by anomalous X-ray scattering coupled with reverse Monte Carlo simulation. *Corrosion Sci.,* 48(6): 1571-1584.

Lado-Touriño, I. & Tsobnang, F. (2000). Using computational approaches to model hematite surfaces. *Computational Mater. Sci.,* 17(2-4): 243-248.

Lattuada, M. & Hatton, T.A. (2006). Functionalization of monodisperse magnetic nanoparticles. *Langmuir,* 23(4): 2158-2168.

Laurent, S., Forge, D., Port, M., Roch, A., Robic, C., Eliat, L.V. & Muller, R.N. (2008). Magnetic iron oxide nanoparticles: Synthesis, stabilization, vectorization physicochemical characterizations and biological applications. *Chem. Rev.,* 108: 2064-2110.

Lee, D.-D. & Choi, D.-H. (1990). Thick-film hydrocarbon gas sensors. *Sens. Actuators B,* 1(1-6): 231-235.

Lee, J., Isobe, T. & Senna, M. (1996). Preparation of ultrafine Fe_3O_4 particles by precipitation in the presence of PVA at high pH. *J. Colloid Interface Sci.,* 177(2): 490-494.

Lee, Y., Lee, J., Bae, C.J., Park, J.G., Noh, H.J., Park, J.H. & Hyeon, T. (2005). Large-scale synthesis of uniform and crystalline magnetite nanoparticles using reverse micelles as nanoreactors under reflux conditions. *Adv. Funct. Mater.,* 15(3): 503-509.

Lenz, J., Campo, B.C., Alvarez, M. & Volpe, M.A. (2009). Liquid phase hydrogenation of [alpha],[beta]-unsaturated aldehydes over gold supported on iron oxides. *J. Catal.,* 267(1): 50-56.

Li, Y., Zhou, Z., Yu, G., Chen, W., & Chen, Z. (2010), CO catalytic oxidation on iron-embedded graphene: computational quest for low-cost nanocatalysts, *J Phys. Chem. C*, 114: 6250-6254.

Li, Z., Chen, H., Bao, H. & Gao, M. (2004). One-pot reaction to synthesize water-soluble magnetite nanocrystals. *Chem. Mater.,* 16(8): 1391-1393.

Li, Z., Lai, X., Wang, H., Mao, D., Xing, C. & Wang, D. (2009). Direct hydrothermal synthesis of single-crystalline hematite nanorods assisted by 1,2-propanediamine. *Nanotechnology,* 20: 1-9.

Liong, M., Lu, J., Kovochich, M., Xia, T., Ruehm, S.G., Nel, A.E., Tamanoi, F. & Zink, J.I. (2008). Multifunctional inorganic nanoparticles for imaging, targeting, and drug delivery. *ACS Nano,* 2(5): 889-896.

Liu, H., Wei, Y., Li, P., Zhang, Y. & Sun, Y. (2007). Catalytic synthesis of nanosized hematite particles in solution. *Mater. Chem. Phys.,* 102(1): 1-6.

López-Quintela, M.A. & Rivas, J. (1993). Chemical Reactions in Microemulsions: A Powerful Method to Obtain Ultrafine Particles. *J. Colloid and Interface. Sci.,* 158(2): 446-451.

Lu, A.H., Salabas, E. & Schüth, F. (2007). Magnetic Nanoparticles: Synthesis, Protection, Functionalization, and Application. *Angew. Chem. Int. Ed.,* 46(8): 1222-1244.

Lu. J., Yang. S., Ng, K.M., Su, C.H.,Yeh, C.S., Wu, Y.N. & Shieh, D.B. (2006). Solid-State synthesis of monocrystalline iron oxide nanoparticle-based ferrofluid suitable for magnetic resonance imaging contrast application. *Nanotechnology,* 17: 5812-5820.

Lyon, J.L., Fleming, D.A., Stone, M.B., Schiffer, P. & Williams, M.E. (2004). Synthesis of Fe oxide core/Au shell nanoparticles by iterative hydroxylamine seeding. *Nano Lett.,* 4(4): 719-723.

Ma, X.Y., Liu, L., Jin, J.J., Stair, P.C., & Ellis, D.E. (2006), Experimental and theoretical studies of adsorption of CH_3 center dot on alpha-Fe_2O_3(0001) surfaces. *Surf. Sci*., 600: 2874-85.

Mahmoudi, M., Simchi, A., Milani, A.S. & Stroeve, P. (2009). Cell toxicity of superparamagnetic iron oxide nanoparticles. *J. Colloid and Interface Sci.,* 336(2): 510-518,0021-9797.

Mammeri, F., Bourhis, E.L., Rozes, L. & Sanchez, C. (2005). Mechanical properties of hybrid organic-inorganic materials. *J. Mater. Chem.,* 15(35-36): 3787-3811.

Martin, A.L., Bernas, L.M., Rutt, B.K., Foster, P.J. & Gillies, E.R. (2008). Enhanced cell pptake of superparamagnetic iron oxide nanoparticles functionalized with dendritic guanidines. *Bioconjugate Chem.,* 19(12): 2375-2384.

Mason, S.E., Iceman, C.R., Tanwar, K.S., Trainor, T.P., & Chaka, A.M. (2009). Pb(II) adsorption on isostructural hydrated alumina and hematite (0001) surfaces: A DFT study, *J. Phys. Chem. C*, 113: 2159-2170.

Massart, R. (1981). Preparation of aqueous magnetic liquids in alkaline and acidic media. *IEEE Trans Magn MAG*, I7: 1247-1248.

Milone, C., Crisafulli, C., Ingoglia, R., Schipilliti, L. & Galvagno, S. (2007). A comparative study on the selective hydrogenation of [alpha],[beta] unsaturated aldehyde and ketone to unsaturated alcohols on Au supported catalysts. *Catal. Today,* 122: 341-351.

Mohapatra, M. & Anand, S. (2010), Synthesis and applications of nano-structured iron xxides/hydroxides – A Review. *Int. J. Eng. Sci. and Tech.,* 2(8): 127-146.

Mohapatra, S., Pramanik, N., Mukherjee, S., Ghosh, S. & Pramanik, P. (2007). A simple synthesis of amine-derivatised superparamagnetic iron oxide nanoparticles for bioapplications. *J. Mater. Sci.,* 42(17): 7566-7574.

Molday, R.S. & Mackenzie, D. (1982). *J. Immun. Methods,* 52: 353-367.

Morais, P.C., Oliveira, A.C., Tronconi, A.L., Goetze, T. & Buske, N. (2003). Photoacoustic spectroscopy: a promising technique to investigate magnetic fluids. *IEEE Trans. Magn.,* 39(5): 2654-2656.

Morber, J.R, Ding, Y., Haluska, M. S., Li, Y., Liu, J. P., Wang, Z. L. & Snyder, R. L. (2006). *J. Phys. Chem. B,* 110*: 21672.*

Mornet, S., Vasseur, S., Grasset, F. & Duguet, E. (2004). Magnetic nanoparticle design for medical diagnosis and therapy. *J. Mater. Chem.,* 14(14): 2161-2175.

Morrissey, J. & Guerinot, M.L. (2009). Iron uptake and transport in plants: The good, the bad, and the ionome. *Chem. Rev.,* 109(10): 4553-4567.

Nakatani, Y. & Matsuoka, M. (1983). Some Electrical Properties of γ-Fe_2O_3 Ceramics. *Jpn. J. Appl. Phys.,* 22: 232-239.

Neri, G., Bonavita, A., Galvagno, S., Siciliano, P. & Capone, S. (2002). CO and NO_2 sensing properties of doped-Fe_2O_3 thin films prepared by LPD. *Sens. Actuators B,* 82(1): 40-47,0925-4005.

Pascal C., Pascal J.L., Favier F., Elidrissi Moubtassim M.L. & Payen C. (1999). Electrochemical synthesis for the control of γ-Fe_2O_3 nanoparticle size. Morphology, microstructure, and magnetic behavior. *Chem. Mater.* 11: 141-147.

Pedro, T. Morales, M. del P., Veintenillas-verdaguer, S., Gonzalez-carreno, T. & Serma, C.J. (2003). The preparation of magnetic nanoparticles for applications in biomedicine. *J. Phys. D: Appl. Phys.,* 36(13): R182.

Pinho, S.L.C., Pereira, G.A., Voisin, P., Kassem, J., Bouchaud, V.r., Etienne, L., Peters, J.A., Carlos, L., Mornet, S.p., Geraldes, C.F.G.C., Rocha, J.O. & Delville, M.-H. (2010). Fine tuning of the relaxometry of γ-Fe_2O_3@SiO_2 nanoparticles by tweaking the silica coating thickness. *ACS Nano,* 4(9): 5339-5349.

Pisanic Ii, T.R., Blackwell, J.D., Shubayev, V.I., Fiñones, R.R. & Jin, S. (2007). Nanotoxicity of iron oxide nanoparticle internalization in growing neurons. *Biomater.* 28(16): 2572-2581.

Rockenberger, J., Scher, E.C. & Alivisatos, A.P. (1999). A new nonhydrolytic single-precursor approach to surfactant-capped nanocrystals of transition metal oxides. *J. Am. Chem. Soc.,* 121(49): 11595-11596.

Rohrbach, A., Hafner, J., & Kresse, G. (2004). Ab initio study of the (0001) surfaces of hematite and chromia: Influence of strong electronic correlations. *Phys. Rev. B*, 70: 125426.

Rollmann, G., Rohrbach, A., Entel, P. & Hafner, J. (2004), First-principles calculation of the structure and magnetic phases of hematite. *Phys. Rev. B,* 69: 165107.

Sahu, K.K., Rath, C., Mishra, N.C. & Anand, S. (1997). Microstructural and magnetic studies on hydrothermally prepared hematite. *J. Colloid Interface Sci.,* 185(2): 402-410.

Scirè, S., Crisafulli, C., Minicò, S., Condorelli, G.G. & Di Mauro, A. (2008). Selective oxidation of CO in H_2-rich stream over gold/iron oxide: An insight on the effect of catalyst pretreatment. *J. Molecular Catal. A: Chem.* 284(1-2): 24-32.

Sivula, K., Zboril, R., Le Formal, F., Robert, R., Weidenkaff, A., Tucek, J., Frydrych, J. & Gratzel, M. (2010). Photoelectrochemical water splitting with mesoporous hematite prepared by a solution-based colloidal approach. *J. Am. Chem. Soc.,* 132(21): 7436-7444.

Soler, M.A, Alcantara, G.B., Soares, F.Q., Viali, W.R., Sartoratto, P.P., Fernandez, J.R., da Silva, S.W., Garg, V.K., Oliveira, A.C. & Morais, P.C. (2007). Study of molecular surface coating on the stability of maghemite nanoparticles. *Surf. Sci.,* 601(18): 3921-3925.

Son, S.J., Reichel, J., He, B., Schuchman, M. & Lee, S.B. (2005). Magnetic nanotubes for magnetic-field-assisted bioseparation, biointeraction, and drug delivery. *J. Am. Chem. Soc.,* 127(20): 7316-7317.

Sousa, M.H., Rubim, J.C., Sobrinho, P.G. & Tourinho, F.A. (2001). Biocompatible magnetic fluid precursors based on aspartic and glutamic acid modified maghemite nanostructures. *J. Magn. Magn. Mater.,* 225(1-2): 67-72.

Sun, Q., Reddy, Marquez, M., Jena, P., Gonzalez, C. & Wang, Q. (2007). Theoretical Study on Gold-Coated Iron Oxide Nanostructure: Magnetism and Bioselectivity for Amino Acids. *J. Phys. Chem. C,* 111(11): 4159-4163.

Sun, S., Zeng, H., Robinson, D.B., Raoux, S., Rice, P.M., Wang, S.X. & Li, G. (2003). Monodisperse MFe_2O_4 (M = Fe, Co, Mn) nanoparticles. *J. Am. Cer. Soc.,* 126(1): 273-279.

Sun, S. & Zeng, H. (2004). Size-controlled synthesis of magnetite nanoparticles. *J. Am. Cer. Soc.,* 124: 8204-8205.

Tao, S., Liu, X., Chu, X. & Shen, Y. (1999). Preparation and properties of [gamma-Fe_2O_3 and Y_2O_3 doped gamma-Fe_2O_3 by a sol-gel process. *Sens. Actuators B,* 61(1-3): 33-38.

Tartaj, P., González-Carreño, T. & Serna, C.J. (2001). Single-step nanoengineering of silica coated maghemite hollow spheres with tunable magnetic properties. *Adv. Mater.,* 13(21): 1620-1624.

Teja, A.S. & Koh, P.-Y. Synthesis, properties, and applications of magnetic iron oxide nanoparticles. *Progress in Crystal Growth and Characterization of Mater.,* 55(1-2): 22-45.

Zhang, T., Luo, H, Zeng, H, Zhang, R. & Shen, Y.(1996). Synthesis and gas-sensing characteristics of high thermostability γ-Fe_2O_3 powder. *Sens. Actuators B,* 32: 181-184.

Tong, S., Hou, S., Zheng, Z., Zhou, J. & Bao, G. (2010). Coating optimization of superparamagnetic iron oxide nanoparticles for high T2 relaxivity. *Nano Lett.*, 10: 1530-6984.

Tristão, J., Ardisson, J., Sansiviero, M. & Lago, R. (2010). Reduction of hematite with ethanol to produce magnetic nanoparticles of Fe_3O_4 coated with carbon. *Hyperfine Interactions,* 195(1): 15-19.

Tristão, J.C., Silva, A.A., Ardisson, J.D. & Lago, R. (2009). Magnetic nanoparticles based on iron coated carbon produced from the reaction of Fe_2O_3 with CH_4: a Mössbauer study. LACAME 2008. J. Desimoni, C. P. Ramos, B. Arcondo, F. D. Saccone and R. C. Mercader, Springer Berlin Heidelberg: 21-25.

Varanda, L.C., Morales, M.P., Jafelicci, J.M. &Serna, C.J. (2002). Monodispersed spindle-type goethite nanoparticles from FeIII solutions. *J. Mater. Chem.,* 12(12): 3649-3653.

Vidal-Vidal, J., Rivas, J. & López-Quintela, M.A. (2006). Synthesis of monodispersed maghemite nanoparticles by the microemulsion method. *Colloids Surf. A,* 288: 44-51.

Vijayakumar, R., Koltypin, Y., Xu, X.N., Yeshurun, Y., Gedanken, A. & Felner, I. (2001). Fabrication of magnetite nanorods by ultrasonic irradiation. *J. Appl. Phys.*, 89, 6324-28.

Wang, H., Brandl, D.W., Le, F., Nordlander, P. & Halas, N.J. (2006). Nanorice: A hybrid plasmonic nanostructure. *Nano Lett.,* 6(4): 827-832.

Wang, L., Luo, J., Maye, M., Fan, Q., Rendeng, Q., Engelhard, M.E., Wang, C., Lin, Y. & Zhong, C.J. (2005). Iron oxide–gold core–shell nanoparticles and thin film assembly. *J. Mater. Chem.,* 15: 1821-1832

Wang, Z., Guo, H., Yu, Y. & He, N. (2006). Synthesis and characterization of a novel magnetic carrier with its composition of Fe_3O_4/carbon using hydrothermal reaction. *J. Magn. Magn. Mater.,* 302(2): 397-404.

Weckler, B. & Lutz, H.D. (1998) Lattice vibration spectra. Part XCV. Infrared spectroscopic studies on the iron oxide hydroxides goethite ([alpha]), akaganéite ([beta]), lepidocrocite ([gamma]), and feroxyhite ([delta]). *European J. Solid State and Inorg. Chem.,* 35(8-9): 531-544.

Wong, K., Zeng, Q.H. &Yu, A.B. (2011). Electronic structure of metal (M = Au, Pt, Pd, or Ru) bilayer modified α-Fe_2O_3(0001) surfaces. *J. Phys. Chem. C,* 115(11): 4656-4663.

Wu, W., He, Q. & Jiang, C. (2008). Magnetic iron oxide nanoparticles: Synthesis and surface functionalization strategies. *Nanoscale Res. Lett.,* 3: 397-415

Xu, Z., Hou, Y. & Sun, S. (2007). Magnetic core/shell Fe_3O_4/Au and Fe_3O_4/Au/Ag nanoparticles with tunable plasmonic properties. *J. Am. Chem. Soc.,* 129(28): 8698-8699.

Yang, Z., Lu, Z., Luo, G. & Hermansson, K. (2007), Oxygen vacancy formation energy at the Pd/CeO_2(111) interface. *Phys. Lett. A*, 369: 132-139.

Ye, Q.-L., Kozuka, Y., Yoshikawa, H., Awaga, K., Bandow, S. & Iijima, S. (2007). Effects of the unique shape of submicron magnetite hollow spheres on magnetic properties and domain states. *Physical Review B,* 75(22): 224404

Yue, J., Jiang, X.C. & Yu, A.B. (2010). Molecular dynamics study on the growth mechanism of goethite ([alpha]-FeOOH) nanorods. *Solid State Sciences,* 13(1): 263-270.

Yue, J., Jiang, X.C. & Yu, A.B. (2011). Experimental and theoretical study on the β-FeOOH nanorods: growth and conversion. *J. Nanoparticle Res.,* 13(9): 3961-3974.

Yue, J., Jiang, X.C., Zeng, Q. & Yu, A.B. (2010). Experimental and numerical study of cetyltrimethylammonium bromide (CTAB)-directed synthesis of goethite nanorods. *Solid State Sciences,* 12(7): 1152-1159.

Yue, J., Jiang, X.C. & Yu, A.B. (2011). Molecular Dynamics Study on Au/ Fe_3O_4 Nanocomposites and Their Surface Function toward Amino Acids. *J. Phys. Chem. B.*, 115:11693-11699.

Zeng, Q.H., Yu, A.B. & Lu, G.Q. (2008). Multiscale modeling and simulation of polymer nanocomposites. *Progress in Polymer Sci.,* 33(2): 191-269.

Zhai, Y., Zhai, J., Wang, Y., Guo, S., Ren, W. & Dong, S. (2009). Fabrication of iron oxide core/shell submicrometer spheres with nanoscale surface roughness for efficient surface-enhanced Raman scattering. *J. Phys. Chem. C* 113(17): 7009-7014.

Zhang, J., Liu, X., Guo, X., Wu, S. & Wang, S. (2010). A general approach to fabricate diverse noble metal (Au, Pt, Ag, Pt/Au)/Fe_2O_3 hybrid nanomaterials. *Chem.–Eur. J.,* 16(27): 8108-8116.

Zhang, S., Niu, H., Hu, Z., Cai, Y. & Shi, Y. (2010). Preparation of carbon coated Fe_3O_4 nanoparticles and their application for solid-phase extraction of polycyclic aromatic hydrocarbons from environmental water samples. *J. Chromatography A,* 1217(29): 4757-4764.

Zhang, W.M., Wu, X.L., Hu, J.S., Guo, Y.G. & Wan, L.J. (2008). Carbon coated Fe_3O_4 nanospindles as a superior anode material for lithium-ion batteries. *Adv. Funct. Mater.,* 18(24): 3941-3946.

Zhang, Z., Zhang, Q., Xu, L. & Xia, Y.-B. (2007). Preparation of nanometer γ-Fe_2O_3 by an electrochemical method in non-aqueous medium and reaction dynamics. *Synthesis and Reactivity in Inorg. Metal-Org. and Nano-Metal Chem.*, 37: 53–56.

Zhong, J. & Adams, J.B. (2008). Adhesive metal transfer at the Al(111)/a-Fe_2O_3(0001) interface: a study with ab initio molecular dynamics, modelling and simulation. *Mater. Sci. and Eng*., 16: 085001(9 pages).

Zhong, Z., Ho, J., Teo, J., Shen, S. & Gedanken, A. (2007). Synthesis of porous α-Fe_2O_3 nanorods and deposition of very small gold particles in the pores for catalytic oxidation of CO. *Chem. Mater.,* 19(19): 4776-4782.

Zhong, Z., Lin, J., Teh, S.P., Teo, J. & Dautzenberg, F.M. (2007). A rapid and efficient method to deposit gold particles onto catalyst supports and its application for CO oxidation at low temperatures. *Adv. Funct. Mater.,* 17(8): 1402-1408.

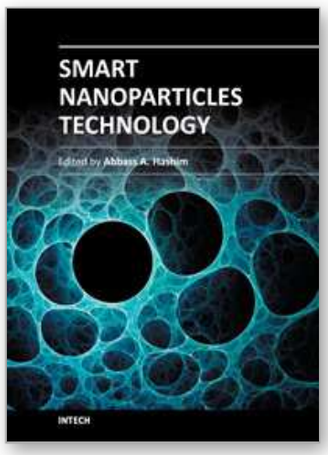

Smart Nanoparticles Technology

Edited by Dr. Abbass Hashim

ISBN 978-953-51-0500-8
Hard cover, 576 pages
Publisher InTech
Published online 18, April, 2012
Published in print edition April, 2012

In the last few years, Nanoparticles and their applications dramatically diverted science in the direction of brand new philosophy. The properties of many conventional materials changed when formed from nanoparticles. Nanoparticles have a greater surface area per weight than larger particles which causes them to be more reactive and effective than other molecules. In this book, we (InTech publisher, editor and authors) have invested a lot of effort to include 25 most advanced technology chapters. The book is organised into three well-heeled parts. We would like to invite all Nanotechnology scientists to read and share the knowledge and contents of this book.

How to reference

In order to correctly reference this scholarly work, feel free to copy and paste the following:

Jeffrey Yue, Xuchuan Jiang, Yusuf Valentino Kaneti and Aibing Yu (2012). Experimental and Theoretical Study of Low-Dimensional Iron Oxide Nanostructures, Smart Nanoparticles Technology, Dr. Abbass Hashim (Ed.), ISBN: 978-953-51-0500-8, InTech, Available from: http://www.intechopen.com/books/smart-nanoparticles-technology/experimental-and-theoretical-studies-on-low-dimensional-iron-oxide-nanostructures-

INTECH
open science | open minds

InTech Europe
University Campus STeP Ri
Slavka Krautzeka 83/A
51000 Rijeka, Croatia
Phone: +385 (51) 770 447
Fax: +385 (51) 686 166
www.intechopen.com

InTech China
Unit 405, Office Block, Hotel Equatorial Shanghai
No.65, Yan An Road (West), Shanghai, 200040, China
中国上海市延安西路65号上海国际贵都大饭店办公楼405单元
Phone: +86-21-62489820
Fax: +86-21-62489821

IntechOpen